Multifunctional Leaky-Wave Antenna With Tailored Radiation and Filtering Characteristics Based on Flexible Mode-Control Principle

DONGZE ZHENG (Graduate Student Member, IEEE) AND KE WU (Fellow, IEEE)

Poly-Grames Research Center, Polytechnique Montreal, Montreal, QC H3T 1J4, Canada

CORRESPONDING AUTHOR: D. ZHENG (e-mail: dongze.zheng@polymtl.ca)

ABSTRACT In this paper, a class of single-layered multifunctional leaky-wave antennas (LWAs) with flexibly engineered radiation and filtering characteristics are proposed and demonstrated for microwave and millimeter-wave applications. Radiating discontinuities (RDs) exhibiting multiple resonances while particularly possessing flexible model-control capability are exploited to accomplish such design freedoms and multifunctionalities of LWAs. By properly engineering the resonance characteristics of RDs under the mode-control principle, the attenuation constant of relevant LWAs can not only be freely tailored for diverse beamwidth/directivity requirements, but also simultaneously maintain a flat frequency response for radiation stability. Meanwhile, controllable filtering behaviors can be obtained as well by the LWAs thanks to the transmission zeros introduced by resonances. Consequently, both the radiation and filtering performances of LWAs can be adequately tailored by taking advantage of the mode-control capability of RDs. Under this design concept, two types of LWAs based on substrate-integrated waveguide and microstrip techniques are respectively developed for different system integration platforms. The substrate-integrated waveguide LWA whose unit cells consist of different longitudinal slots is firstly examined. Additionally, the microstrip LWA, which depends on stub-loaded resonators, is further investigated. The proposed two LWAs are all with flexible engineered electrical behaviors, single-layer, low-cost, and easy integration; they may be a potential candidate for various system applications such as 5G communication and Internet of Vehicles.

INDEX TERMS 5G, beam-scanning, design flexibility, filtering antenna, Internet of Things (IoT), Internet of Vehicles (IoV), leaky-wave antenna (LWA), mode-control, multimode resonator (MMR), multifunctionalities, system integration.

I. INTRODUCTION

LEAKY-WAVE antennas (LWAs) have been well-known for the unique frequency-driven beam-scanning capability, thanks to which they may find potential in system applications such as wireless communications, real-time spectrogram analyzers, and automotive radar sensors [1]–[2]. Most LWAs physically manifest periodic appearances and are normally realized by periodically loading radiating discontinuities (RDs) along the host guides or transmission lines (TLs). Among these LWAs, some using the fundamental space-harmonic for radiation are referred to as quasi-uniform LWAs [3]–[9], while others employing the higher-order (e.g., −1st-order) counterparts are termed periodic LWAs [10]–[24]. Different from the above-mentioned

classifications that are conventionally based on the radiating harmonics or geometry, LWAs, however, can also be classified into two basic groups from the perspective of resonance behaviors of RDs, i.e., single-mode resonator (SMR) and multimode resonator (MMR) [24]. This is because various kinds of resonant structures are commonly used as RDs to construct LWAs, such as slots [4]–[9], [13]–[15], stubs [10]–[12], dipoles [16]–[18], patches [19]–[21], and composite structures [22]–[24], etc. Notably, those RDs are not just limited to enable host TLs radiative; their resonance characteristics certainly have a significant influence on the complex propagation constants of the leaky modes or space-harmonics. Thus, they critically impact the electrical performances of LWAs, such as the realization of
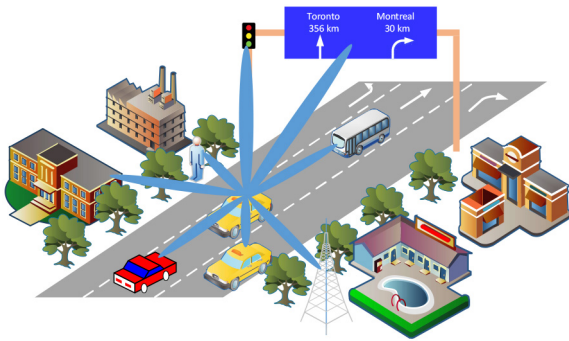
FIGURE 1. A simplified illustration of 5G-enabled IoV.

FIGURE 2. Generalized equivalent circuit models of a periodic LWA. (a) Series loading type. (b) Shunt-loading type. The radiating discontinuities (i.e., Z_{rd} and Y_{rd}) can represent an SMR or MMR.

high directivity [10], stable radiation [11], [12], [22], [24], and rapid beam-scanning [6], [15], [23], etc.

As one of the most significant application scenarios of Internet of Things (IoT), Internet of Vehicles (IoV) has recently experienced an unprecedented development thanks to the emergence of 5G technologies [25]–[27]. 5G-enabled IoV (5G-IoV) makes vehicle-to-everything (V2X) realizable with significant benefits of latency, data speed, reliability, and security, thanks to which autonomous driving developments will become practicable in the short future. As a critical radio frequency (RF) frond-end component in such 5G applications (i.e., IoV), antennas implemented on the host vehicles should be capable of providing a specific narrow and directive beam to each "user" (e.g., other guest vehicles, pedestrians or infrastructures), as shown in Fig. 1. Such required multiple beams (or beam-scanning) are usually realized by complicated beam-forming networks, costly phase shifters, or computationally intensive back-end digital signal processing techniques. Comparatively, beam-scanning simply driven by frequency is a relatively cost-effective and straightforward solution. Due to the features of simple feeding, narrow directive beam, and unique frequency-driven beam-scanning property, LWAs present a promising candidate, which have already been developed for automotive radar sensors [28], [29] and may be deployed for prospective 5G-IoV applications. Nevertheless, a well-designed LWA for potentially practical use should simultaneously have some desirable merits and functionalities, e.g., adequate design freedoms and flexibilities of electrical characteristics (radiation and circuit performances), low-cost, easy fabrication and integration, etc. To be specific, it is of great significance and necessity for an LWA that can be customized in terms of its beamwidth/directivity to meet different practical specifications. Simultaneously, the LWA should also maintain stable beam-scanning performances so as to provide uniform effective isotropically radiated power (EIRP) in the field of view (FoV) of V2X communication. Moreover, it would be better if this LWA can also be equipped with filtering capability to reduce total circuit size and improve overall front-end system performances (e.g., insertion loss, noise figure and dynamic range). Although a singular functionality of LWAs such as radiation stability [11], [12], [22], [24] or
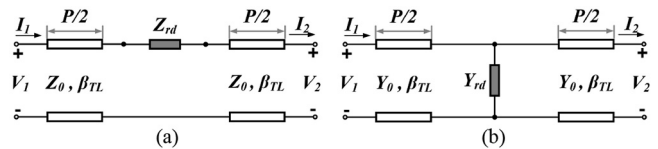
filtering characteristics [30]–[32] can be found in the open literature, no reported works, to the best of the authors' knowledge, have been specially dedicated to combining multifold functionalities such as radiation stability and filtering behavior as well as flexible engineering capability into a single LWA. More critically, practical industrial significance of LWAs such as low-cost and easy fabrication/integration properties should also be simultaneously taken into account aimed for mass-production.

In this work, such kind of LWAs, taking advantage of the flexible mode-control principle of RDs and simple single-layer PCB processing, are developed for microwave and millimeter-wave system applications. The main contribution of this work is reflected on the artful use of MMR-based RDs featuring flexibly controlled modes for LWAs with good design freedoms and multifunctional electrical performances such as manageable beamwidth, controllable bandwidth/filtering characteristics, and stable radiation. Different TL technologies such as substrate-integrated waveguide (SIW) and microstrip are respectively exploited as the host TLs, aimed for diverse system integration platforms. An SIW LWA, whose unit cell consists of different longitudinal slots exhibiting multiple independently controllable resonances, is first to be investigated. Comparatively, an open-circuited stub-loaded resonator (OCSLR) with the similar flexible model-control behavior is subsequently proposed and implemented for a microstrip combline LWA. It is demonstrated that by properly controlling the RD's several resonant modes simultaneously (i.e., the so-called flexible mode-control), the attenuation constant of related LWAs can be freely adjusted during which a stable frequency response of it can always be maintained. This is not only useful for LWAs to realize radiation stability, but also beneficial to accomplish diverse beamwidth specifications as well as wideband behaviors of low side-lobe radiation. On the other hand, strong resonances of the RD will cut off the whole transmission link of relevant LWAs and thus introduce transmission zeros, exhibiting desirable filtering characteristics in the frequency band of LWAs. Due to the multifold benefits such as flexibly engineered radiation and filtering characteristics, single-layer, low-cost, and easy fabrication/integration, the proposed LWAs may find potentials in practical applications such as the 5G communication and IoV.

II. PROBLEM ANALYSIS AND DESIGN PRINCIPLE
For an LWA that is not tapered along its wave-propagation direction, its radiation characteristics can be easily predicted

by its complex propagation constants, namely the attenuation constant α and phase constant β. For a periodic LWA using the -1st order space-harmonic to radiate, its main-beam direction θ_m and 3-dB beamwidth $\Delta\theta$ can be expressed by the following equations [1], [2]

$$\theta_m \simeq \sin^{-1}\left(\frac{\beta}{k_0}\right), \Delta\theta \simeq 5\frac{\alpha/k_0}{\cos(\theta_m)} \qquad (1)$$

where k_0 and λ_0 are the free-space wavenumber and wavelength, respectively. The 3-dB beamwidth $\Delta\theta$ in (1) assumes 90% efficiency provided that there are no material losses, and the remaining 10% of the injected power is absorbed by a matching-load at the end (i.e., matching-load loss). It can be seen from (1) that to realize various beamwidths of an LWA customized for different application scenarios, its attenuation constant should be altered accordingly. It has already been demonstrated in [24] that there is an approximate one-to-one mapping relation between the RD's normalized resistance/conductance and the attenuation constant of the related LWA, which can be expressed as

$$\alpha \simeq -\ln\left[1 - re\left(\frac{Z_{\text{rd}}}{Z_0}\right)\right]/2P \text{ or } -\ln\left[1 - re\left(\frac{Y_{\text{rd}}}{Y_0}\right)\right]/2P, \qquad (2)$$

corresponding to the series-loading and shunt-loading circuit models as shown in Fig. 2(a) and (b), respectively. Z_{rd} and Y_{rd} represent the impedance and admittance of the loaded RDs, while Z_0 and Y_0 denote the characteristic impedance and admittance of the host TLs, respectively. P is the period length of unit cells. According to (1) and (2), two effective approaches can be used to control the attenuation constant or beamwidth of an LWA: change either the absolute resistance/conductance of the RD, or the characteristic impedance/admittance of the host TLs. In general, the realization of various attenuation constants for an LWA is usually realized by resizing the RD and shifting its resonance close to or away from the design frequencies so as to manage its absolute resistance/conductance value. For example, by changing the length of the slot/stub/dipole, the related resonance frequency and thus the attenuation constant can be adjusted to facilitate a low side-lobe design of the LWAs [6], [8], [9], [11], [17]. However, it should be noted that although the attenuation constant can be altered by shifting the resonance frequency of the RD, it is hard for these relevant LWAs to simultaneously hold a flat frequency response of the attenuation constant over the frequency band of interest. Thus, the design freedoms and flexibilities as well as the electrical performances of LWAs have to be compromised to some extent. This is especially true for SMR-related LWAs [24]. To make matters worse, a further deterioration of radiation fluctuation would be encountered when requiring a larger attenuation constant in these LWAs. The reason for this is easily understood since such a situation usually needs to shift the RD's resonance closer to the design frequency band. Thus, a more dramatic variation would occur for the resistance/conductance properties
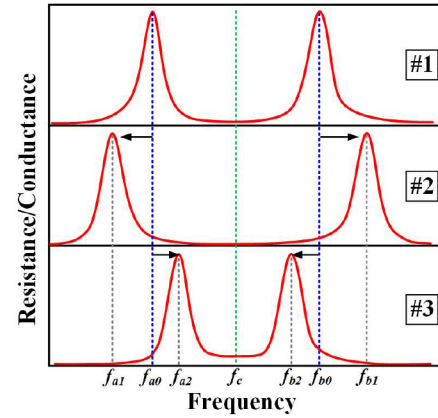

FIGURE 3. Mode-control principle for the design flexibilities and multifunctionalities of LWAs. Curve peaks can represent either series- or shunt-resonances, corresponding to the conductance or resistance case accordingly. While the #1 is referred to as the reference, the #2 is with an increased frequency distance of resonances and the #3 has the reverse situation.

of such an RD as well as for the radiation behaviors of associated LWAs over frequencies.

Recall that in our RF/microwave communities resonance behaviors are always crystallized in a periodic manner over the frequency domain thanks to the periodic essence of time-harmonic electromagnetics and specific boundary conditions [33]. Because of this, a simple resonant structure such as a dipole, slot, stub, and patch naturally possesses several resonant modes over frequency as simply illustrated in Fig. 3, and these multiple resonances may be simultaneously used for operations such as the design of multiband or wideband antennas [34]. Nevertheless, in most cases, only one of these modes (usually the fundamental one) is used for operations because it is easier to manipulate only one mode at a time compared to the simultaneous control of multiple modes. This partially explains why most of resonant structures are usually under the treatment of an SMR in some typical applications like those LWAs with a low side-lobe design [6], [8], [9], [11], [17]. Interestingly, multiple simple structures with each donating only one of its modes can also be combined to constitute a composite structure presenting MMR behaviors like Fig. 3, such as the well-known magneto-electric dipole and aperture-coupled patch [22], [24], [35]. Notably, even though MMR-based RDs can be adopted to construct LWAs for radiation stability like the works in [22] and [24], the design freedoms and flexibilities of diversified beamwidths while maintaining the radiation stability are still difficult to be simultaneously realized, since this requires that several resonances of the RD could be flexibly controlled to stabilize the normalized resistant/conductance curve over the frequency band of interest as revealed in Fig. 3. Obviously, to realize a changeable resistance/conductance value while simultaneously keeping its flat frequency response, the two relevant strong resonances (i.e., curve peaks in Fig. 3) of the MMR-based RD should be engineered on the beat. In other words, the flexible-mode control capability should be equipped for
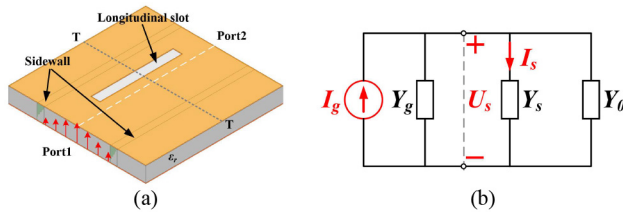
FIGURE 4. Traditional longitudinally slotted SIW LWA unit cell with a single slot [36]. (a) Geometry. (b) Norton equivalent circuit model. The longitudinal slot is simply modeled as a series *RLC* resonator that is parallel-connected into the SIW, similar to Fig. 2(b). In (b), *Ig* denotes the current source, and it also represents the transverse currents flowing on the broad wall of the SIW. Y_g is the source admittance, which is equal to the characteristic admittance of the SIW, i.e., Y_0. The slot's admittance is represented as Y_S.

FIGURE 5. Longitudinally slotted SIW LWA unit cell with two different slots. (a) Unilateral and (b) bilateral (proposed) arrangements with respect to the longitudinal centerline. Both slots resonate at a half-wavelength mode.

the RD. Since the resistance/conductance value is normally related to the frequency locations of the two strong resonances, they can be controlled to be far away from the center frequency to lower the resistance/conductance value of the RD and thus the attenuation constant according to (2). Contrastively, improved radiation leakage can be achieved by shorting the frequency distance of such two modes. In both cases, stable frequency response can always be held if frequency locations of the two modes are kept symmetrical about the center frequency. It is interesting to mention that another significant benefit of the flexible mode-control principle illustrated in Fig. 3 can be found in LWAs' low side-lobe design over a wide bandwidth. This is because in this case the attenuation constant distribution along the leaky structure according to a specific aperture illumination would be frequency-independent, which cannot be meet by most of current low-side lobe designs [6], [8], [9], [11], [17]. On the other hand, when relating the resonance behaviors illustrated in Fig. 3 to the LWAs' equivalent circuits shown in Fig. 2 (a) or (b), it can be found that the two strong resonances, which represent shunt-resonances in the impedance case or series-resonances in the admittance one, would respectively behave as "open" in Fig. 2(a) or "short" in Fig. 2(b). Thus, such two strong resonances can turn off the energy transmission and produce two relatively symmetrical transmission zeros or stopbands in LWAs [33]. These stopbands can be potentially used to control operating bandwidth of the periodic LWAs. Namely, the operating bandwidth of the periodic LWAs can be flexibly adjusted by resorting to the MMR-based RDs featuring flexible mode-control capability. In conclusion, the resonance behaviors of an RD should have the merit of flexible mode-control capability for prospective LWAs to simultaneously realize stable radiation, manageable beamwidth, and controllable bandwidth/filtering behaviors. This kind of LWAs featuring such design flexibilities and benefits will be investigated and developed in the following sections.

III. ASYMMETRICALLY LONGITUDINAL SHUNT-SLOT-PAIR (ALSSP)-BASED SIW LWA
A. DEVELOPMENT OF THE ALSSP-BASED RD

Fig. 4(a) depicts the geometry of a traditional longitudinally slotted SIW LWA unit cell [36]. Only a single longitudinal slot is etched on the top broad wall of the SIW along
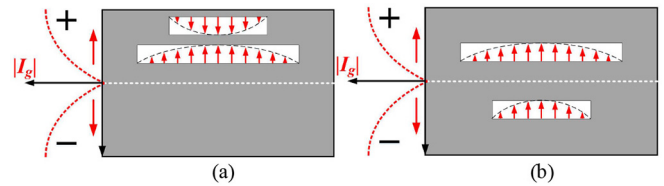
which the dominant TE_{10} mode is assumed to be excited and guided. Radiation occurs when the longitudinal slot is offset from the longitudinal centerline, since transverse currents on the SIW's broad wall would be cut off by the slot. Simplified excitation mechanism of the slot can be explained by the Norton equivalent circuit model, as shown in Fig. 4(b), where the transverse currents behave as a current source and excite the slot resonating at a half-wavelength mode. Notably, the admittance property of the slot is usually characterized as an SMR without exhibiting higher-order modes which are hardly excited under such a slot-excitation-mechanism. Thus, the slot is simply modeled as a series *RLC* resonator that is parallel connected to the host SIW lines, similar as Fig. 2(b). In order to create multiple resonances behaviors in the slot, extra structures must be incorporated with it. For example, planar electric dipole or patch can be additionally attached over the longitudinal slot to form multi-layered composite structures, presenting multiple resonances [22], [24], [35]. However, strong electromagnetic coupling is used as the feeding mechanism in these structures, for which those relevant resonant modes are mutually coupled and cannot be flexibly controlled for operations to some extent, not to mention that such multilayer geometries would bring the cost and fabrication issues in practical applications. Inspired from the excitation mechanism of the longitudinal slot [36] and the works in [37]–[38], multiple longitudinal slots with different dimensions and resonant frequencies can be etched on the SIW. Typically, two slots are taken into account, and thus two arrangements, namely unilateral and bilateral cases, can be deployed as shown in Fig. 5, in which the simplified aperture field and transverse current distributions are also illustrated. For the unilateral case, the two slots will feature oppositely directed aperture field distributions, which can be conveniently expounded by the Norton equivalent circuit shown in Fig. 4(b). Specifically, in the target frequency band (i.e., the band between the two resonances respectively introduced by the two slots), the two slots behave with opposite susceptance behaviors. One is inductive (after its own resonance) while the other is capacitive (before its own resonance) over such a frequency range. They will possess reversely directed electrical potential differences (voltages) and so do their aperture fields since their driven currents share the same direction, as illustrated in Fig. 5(a). Obviously, it is difficult for this unit cell to radiate since most of radiation originated from the two slots cancel
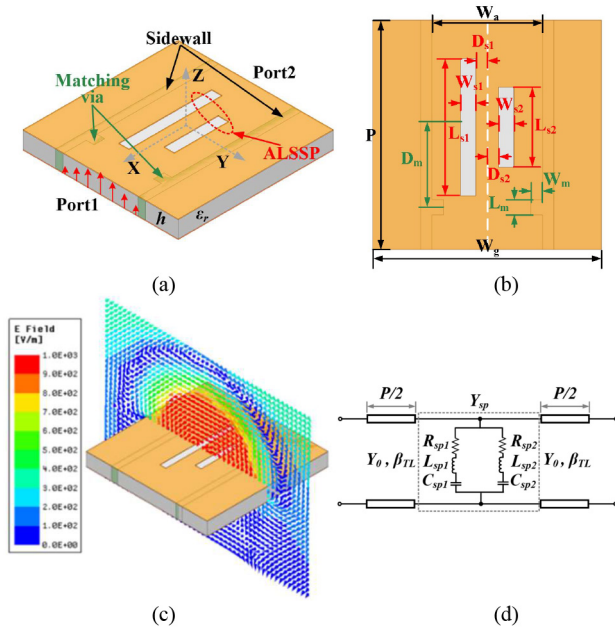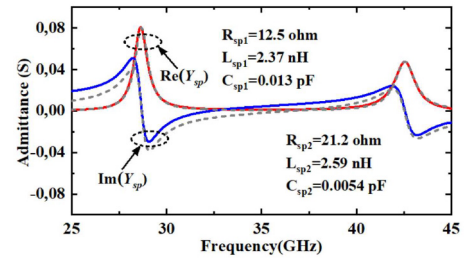
FIGURE 7. Admittance frequency responses of the proposed ALSSP-based RD with respect to full-wave (solid line) and circuit (dash line) simulations.
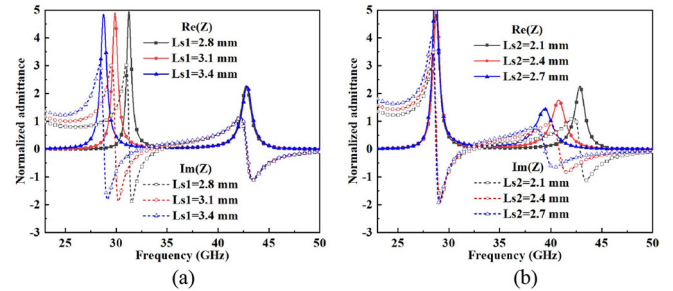
FIGURE 6. ALSSP-based SIW LWA unit cell. (a) 3-D view (not to scale); (b) top view (not to scale); (c) cross-sectional E-filed distribution (35 GHz); (d) equivalent circuit model neglecting the matching vias. The substrate is RT/duroid 6006 with a thickness of 0.635 mm, relative permittivity of 6.45, and loss tangent of 0.0027. Specific dimensions are $P = 4.15$, $W_g = 2.9$, $W_a = 6$, $L_{s1} = 3.4$, $W_{s1} = 0.3$, $D_{s1} = 0.2$, $L_{s2} = 2.1$, $W_{s2} = 0.6$, $D_{s2} = 0.3$, $D_m = 1.96$, $L_m = 0.356$, $W_m = 0.266$, $h = 0.635$, $t = 0.4$ (unit: mm).

FIGURE 8. Dimensional effects of the ALSSP on its normalized admittance behaviors. (a) L_{s1}. (a) L_{s2}. The two studied parameters are the length of the longer and shorter slots, respectively.

each other out. As a comparison, thanks to the reversely directed transverse currents on the two halves of the SIW, the two oppositely signed (susceptance-complementary) slots will embrace the same-directed aperture fields, and this corresponds to the bilateral arrangement as shown in Fig. 5(b). In this case, the two slots can work together as an effective radiator characterized by multiple resonances, as will be exhibited later. Although a similar dual-slot geometry can also be found in [38], more physical insights and extensive characterizations are explored and clarified in this paper in terms of the circuit modeling and radiation mechanism of the structure, as described above and also will be illustrated later. Also note that the research purposes between the two are totally different. Due to the fact that the two slots are different in size and distributed on the two halves of the SIW along the longitudinal centerline and all share the same type of shunt-loading effects on the SIW, the two slots are thus referred to as "asymmetrically longitudinal shunt-slot-pair" (ALSSP).

B. MULTIPLE RESONANCES BEHAVIOR AND FLEXIBLE MODE-CONTROL OF THE ALSSP

The geometry, cross-sectional E-field distribution, and transmission-line equivalent circuit model of the proposed ALSSP-based SIW LWA unit cell can be found in Fig. 6. Note that a pair of matching vias are embedded into the unit cell for an open-stopband suppression [24]. The simulated cross-sectional E-field distribution of the unit cell is consistent with Fig. 5(b), illustrating that radiated fields emanated

from the two slots are constructively superposed to form effective radiation that interestingly resembles a rectangular patch antenna's radiation mechanisms, i.e., equivalent two-element slot array [34]. In Fig. 6(d), each longitudinal slot of the ALSSP is simply modeled as a series RLC resonator, and the full-wave and circuit simulation results in terms of the ALSSP's admittance are illustrated in Fig. 7. The circuit simulation results are in a reasonably good agreement with their full-wave counterparts, and both exhibit multiple resonances behavior. Values of those circuit components (R_{sp1}, L_{sp1}, C_{sp1} for the long slot, while R_{sp2}, L_{sp2}, and C_{sp2} for the short slot) are obtained by a curve-fitting approach with the help of Advanced Design System (ADS) software. Notably, apart from the two series-resonances that are individually introduced by the two slots, there is an additional shunt-resonance between the two. The reason for its occurrence can be explained using the ALSSP's equivalent circuit model shown in Fig. 6(d). Since the two slot resonator-branches have complementary susceptance properties in the target frequency range as mentioned previously, the inductive slot (long slot) will compensate the capacitive slot (short slot) in terms of their susceptances at one specific frequency point, at which the whole resonator circuit tank (i.e., ALSSP) will satisfy the shunt-resonance condition. Fig. 8 depicts the dimensional effects of the ALSSP on its normalized admittance performances. The two studied parameters L_{s1} and L_{s2} represent the length of the long and short slots, respectively. It is clearly seen that the two series-resonances can be controlled independently, i.e., flexible mode-control capability. Specifically, by increasing L_{s1}, the first series-resonance will be shifted
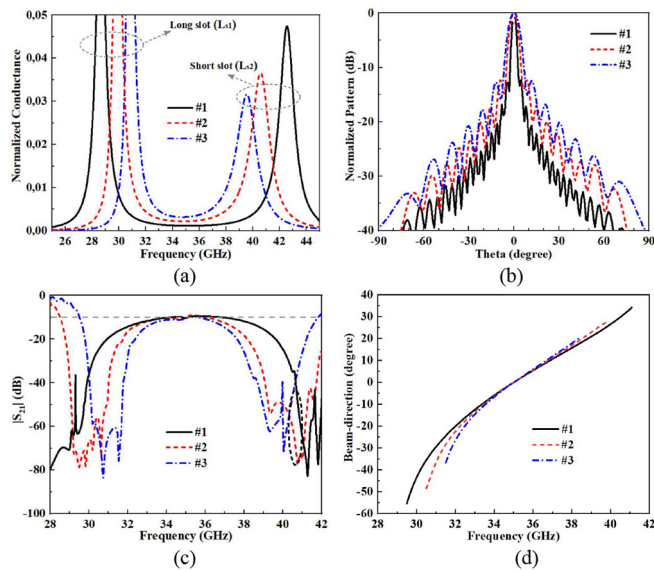
FIGURE 9. Illustration of design flexibilities of the ALSSP-based LWA under mode-control principle. (a) Normalized conductance of ALSSPs. (b) Normalized radiation pattern, (c) $|S_{21}|$ and (d) beam-scanning behaviors of ALSSP-based LWAs. #1, #2 and #3 correspond to different assignments of the slot-length (L_{s1}, L_{s2}), with specific values of (3.4 mm, 2.1mm), (3 mm, 2.4 mm), and (2.8 mm, 2.6 mm), respectively. Also, #1-, #2-, and #3-related LWAs are respectively designed with 36, 19, and 14 unit cells for 90% radiation efficiency.

FIGURE 10. Evolution of microstrip combline antennas. Conventional (a) unilateral and (b) bilateral cases. Proposed (c) case #1 and (d) case #2. Red circles represent radiating edges within a unit cell.

to a lower frequency without influencing the second series-resonance, as shown in Fig. 8(a). A similar phenomenon can also be found with changing L_{s2}, as plotted in Fig. 8(b). The width of the slot is not studied here for brevity since it just shows a little influence on the resonance frequency, beyond our main considerations regarding the flexible mode-control principle [34], [36].

C. CUSTOMIZED CHARACTERISTICS OF THE ALSSP-BASED SIW LWA UNDER FLEXIBLE MODE-CONTROL

In order to verify the claimed benefits of the flexible model-control capability, i.e., design flexibilities of manageable beamwidth and controllable bandwidth/filtering behaviors as well as the radiation stability, resonance behaviors of the ALSSP in terms of its two series-resonances are engineered by changing length of the two slots, i.e., L_{s1} and L_{s2}. Specifically, three groups of (L_{s1}, L_{s2}) are assigned to the ALSSP in such a way that the two series-resonances are with different frequency distances but approximately centered at the design frequency of 35 GHz, as shown in Fig. 9(a) which depicts the normalized conductance of each type of ALSSPs. It can be seen clearly that a shorter frequency distance of the two series-resonances will lead to an increased normalized conductance at the center frequency. This is similar to Fig. 3 and thus will give rise to a wider beamwidth for the relevant LWAs according to (1) and (2), as shown in Fig. 9(b). Herein, each type of the ALSSPs, namely #1, #2, and #3, is periodically loaded onto a lossless SIW line to establish an LWA that has a certain quantity of unit cells for 90% radiation efficiency. Notably, the introduction of matching vias for
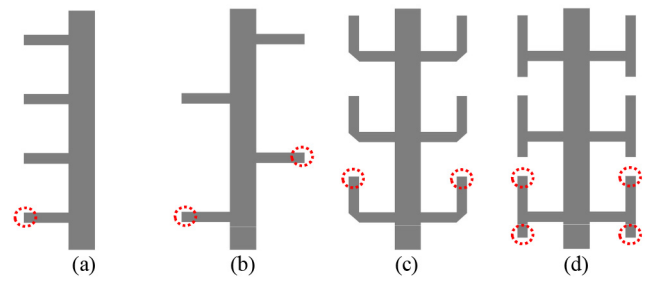
the open-stopband suppression would not significantly influence the previously configured behaviors of the ALSSP. This is due to the fact high-order waveguide modes excited by the matching vias are in a cut-off status and thus are highly attenuated and localized; they hardly reach the slot RD in general [33]. Fig. 9(c) exhibits the $|S_{21}|$ performances of these relevant LWAs, in which stable and symmetrical curve patterns over the middle passband are displayed, thus implying that stable radiation efficiencies can be realized. In this sense, LWAs with diverse beamwidths while simultaneously having stable radiation performances can be realized by taking advantage of the flexible mode-control capability of the ALSSP. Note that a controllable operating passband is also observed in Fig. 9(c), which is sandwiched by two stopbands that are formed by the transmission zeros introduced by the two series-resonances of the ALSSP, as explained previously. Beam-scanning behaviors of these LWAs can be found in Fig. 9(d); it also manifest apparent bandpass characteristics only within which the beam is scanned with frequency. As a result, with the flexible mode-control of the ALSSP, the proposed LWA can provide good design freedoms and flexibilities as well as those multifunctionalities as mentioned previously. Also note that the proposed LWA is only single-layered and can be fabricated using low-cost and simple PCB processing, which is suitable for mass-production in practical use.

IV. EVOLUTIONARY MICROSTRIP COMBLINE LWA BASED ON OPEN-CIRCUITED STUB-LOADED RESONATOR (OCSLR)

A. EVOLUTIONARY DESIGN OF MICROSTRIP COMBLINE LWA USING MULTIPLE RESONANCES

The microstrip open-circuited stub can be interpreted as a microstrip dipole with its one end shorted to the main microstrip line while the other being a radiating edge. Due to its simple geometry and easy fabrication, it is usually used to develop a series of standing-wave antenna arrays [39] and LWAs [10]–[12]. This kind of antennas are often referred to as microstrip "combline" antennas, as shown in Fig. 10(a) and (b) illustrating the two conventional schemes [39]. It is worth noting that the open-circuited stub resonator adopted in these schemes usually has a uniform width or characteristic impedance, and herein it is entitled open-circuited
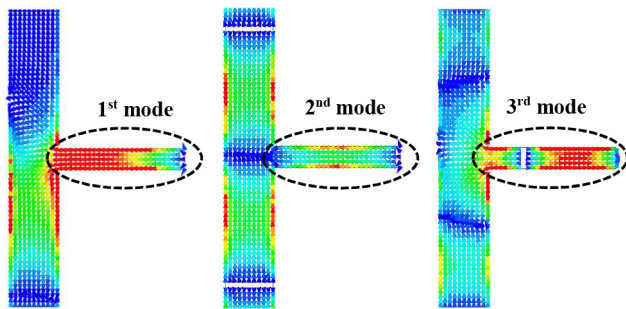
FIGURE 11. Conventional microstrip combline LWA unit cell with respect to its modal current distributions. The first three resonances are exhibited. The 1st and 3rd modes are series-resonances, while the 2nd mode is shunt-resonance. The related equivalent circuit model is the same as Fig. 2(b).

uniform impedance resonator (OCUIR). A unit cell of the conventional microstrip combline LWA [10] and its several modal currents can be seen in Fig. 11. The first three resonant modes respectively correspond to the series-, shunt- and series-resonances, where the electrical length of the stub is approximately equal to one, two, and three quarter-wavelengths accordingly. The equivalent circuit model of the unit cell is the totally same as the one in Fig. 2(b). Due to the natural MMR behaviors of the OCUIR, these resonant modes may be used simultaneously (as mentioned previously) to design microstrip combline LWAs with stable radiation according to the MMR design rules in [24]. Note that this fact has not been recognized and explored in reported similar microstrip stub-based designs [10]–[12]. However, the two conventional schemes shown in Fig. 10(a) and (b) are not symmetrical along the longitudinal direction, which may possibly lead to a high cross-polarization level or asymmetrical cross-sectional radiation pattern [34], [39]. They are also subject to the scanning blind in end-fire directions due to the radiation null of element pattern from such radiating edges of the OCUIR [5]. What is worse, for the conventional bilateral case shown in Fig. 10(b), it would largely suffer from large side-lobes or even grating-lobes in the cross-sectional plane when the working frequency becomes high, since in this case the physical distance between the two bilateral radiating edges would be electrical large that may close to or more than a free-space wavelength. Also note that the common issue of the second-order radiation beams is easily encountered in such an alternatively bilateral arrangement [36], [39]. Consequently, to tackle all the possible issues aforementioned that can also be potentially suffered in [10]–[12], and simultaneously to make use of multiple resonances for stable radiation [24], an evolutionary microstrip combline LWA whose unit cell consists of a pair of symmetrical folded OCUIRs is established as shown in Fig. 10(c). Its specific unit cell geometry can be found in Fig. 12(a) having a trident-like shape. The folded or bend point is located at the center of each OCUIR, where a right-angled corner is delicately cut to reduce the bend discontinuity [39]. Notably, the two radiating edges of the pair of OCUIRs possess identical fringing

field distributions and form a two-element array [40]. The distance between them would never exceed 0.75 free-space wavelength over the whole target frequency band under the MMR design rules even if the employed substrate has a relative permittivity of unity. Thus, the associated LWA will be totally free from side-or grating-lobes in its cross-sectional plane, which cannot be meet by the schemes in Fig. 10(b) and [11]. Also note that in this case, the radiating edge's element pattern is null at the end-fire directions of the cross-sectional plane, which will also play a role in further preventing possible appearances of side- or grating-lobes in this plane. Fig. 12(b) shows the normalized admittance of the pair of OCUIRs. Three resonant modes (two series-resonances and one shunt-resonance) can be clearly observed with a fixed frequency ratio. The overall stub length can be changed to shift frequency locations of the two series-resonances so as to deploy the MMR design rules for the LWAs with stable radiation. For example, we choose 25 GHz as the center/design frequency, and the stub length is altered so that its two series-resonances are approximately centered at this frequency. As for the width of the stub, it can be suitably used to adjust the stub's radiation ability while without significantly influencing its resonance frequencies [33], [39]. For the open-stopband suppression and continuous beam-scanning of the relevant LWA, impedance matching techniques such as a delay line plus a quarter-wavelength transformer can be used [10]. This is shown in Fig. 13 which depicts the normalized complex propagation constants of the LWA together with an inset of the final unit cell. It also shows that a stable attenuation constant is achieved for the unit cell over the target frequency band from 21 to 29 GHz. This stems from the stable frequency response of the normalized conductance of the OCUIR and will lead to the relevant LWA to be equipped with a stable $|S_{21}|$ and radiation efficiency as will be shown later. For demonstration convenience, only 20 unit cells are cascaded to form the proposed OCUIR-based LWA with the fabricated prototype depicted in Fig. 14(a). Good impedance matching exhibited in Fig. 14 (b) indicates that the open-stopband issue has been effectively suppressed, while both stable $|S_{21}|$ of -4.6 ± 0.8 dB and stable radiation efficiency of $59.5\pm4.2\%$ [as shown in Fig. 14(c)] verify the effectiveness of the evolutionary microstrip combline LWA using the natural multiple resonances of the OCUIR for radiation stability.

B. MICROSTRIP COMBLINE LWA BASED ON STUB-LOADED RESONATOR—AN RD WITH FLEXIBLE MODE-CONTROL CAPABILITY

As we have demonstrated previously, an MMR-based RD with flexible mode-control capability is beneficial for LWAs to realize good design freedoms and flexibilities like governable beamwidth and filtering behaviors while simultaneously holding the stable radiation. Although the microstrip combline LWA has been evolved by using multiple resonances of the OCUIR for stable radiation, it is inconvenient
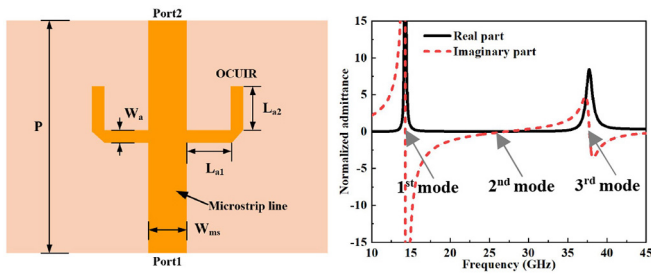
FIGURE 12. (a) Unit cell of the proposed microstrip combline LWA using stub's natural multiple resonances. (b) Normalized admittance of the folded OCUIR. Dimensions of the unit cell are $P = 7.15$ mm, $W_{ms} = 1.12$ mm, $L_{a1} = 1.6$ mm, $L_{a2} = 1.6$ mm, and $W_a = 0.4$ mm. The substrate is RO3035 with a thickness of 0.508 mm, relative permittivity of 3.6, and loss tangent of 0.0015.
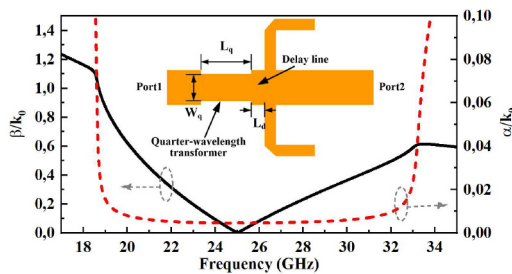

FIGURE 13. Normalized phase and attenuation constants of the proposed LWA. Open-stopband issue is effectively suppressed by using a delay line and quarter-wavelength impedance transformer [10], as shown in the inset. Dimensions of them are $L_d = 0.55$ mm, $L_q = 1.75$ mm, and $W_q = 0.89$ mm.

FIGURE 14. (a) Fabricated prototype of the proposed OCUIR-based microstrip combline LWA. (b) Simulated and measured S-parameters. (c) Simulated radiation efficiency. Radiation efficiency of the OCSLR-based counterpart (this design can be found in Section IV-B) is also plotted in (c) for a comparison.

FIGURE 15. Unit cell of the proposed OCSLR-based microstrip combline LWA. (a) Geometry. (b) Current distributions at the center frequency. The proposed OCSLR consists of a folded OCUIR loaded with a short capacitive stub. Dimensions of the unit cell are $P = 7.25$ mm, $W_{ms} = 1.12$ mm, $L_{b1} = 0.9$ mm, $L_{b2} = 1.8$ mm, $L_{st} = 0.45$ mm, $W_b = 0.4$ mm. The substrate is RO3035 with a thickness of 0.508 mm, relative permittivity of 3.6, and loss tangent of 0.0015.

for this LWA to be versatilely tailored for different application requirements due to the fixed frequency ratio of these resonant modes. Illuminated by [41]–[43] where loaded stubs or pins can be used to perform the flexible mode-control, a short piece of capacitive open-circuited stub is loaded to the folded OCUIR. Thus, an OCSLR-based LWA is established, as shown in Fig. 10(d) and Fig. 15(a). It is necessary to mention that there are two aspects that should be carefully considered when constructing the folded OCSLR. The first is concerned with the selection of the loading point of the short stub for realizing the flexible mode-control. According to the modal current distributions shown in Fig. 11 and the works in [41]–[43], the middle current null point of the 3rd resonance can be loaded with the short capacitive stub for the purpose of realizing an independent control of this mode. Besides, differing from the folded OCUIR described in the last subsection in which the bend point is centrally located and the bend discontinuity is removed, the microstrip bend discontinuity can be artfully used here when folding a straight stub at the middle current null point of 3rd resonance. In this case, the bend discontinuity can cooperate with the loaded capacitive stub to adjust this mode independently, as can be seen in Fig. 16. When the loaded capacitive stub is absent (i.e., $L_{st} = 0$), the folded OCUIR whose bend discontinuity is located at the current null point of the 3rd mode has an obvious lower modal frequency compared to its counterpart that has no bend discontinuity, regarding this resonance. Meanwhile, this resonance can be progressively
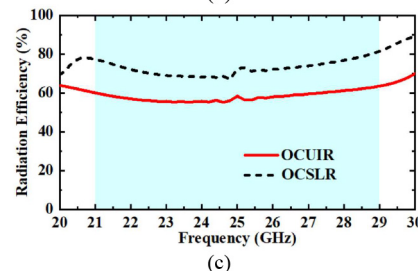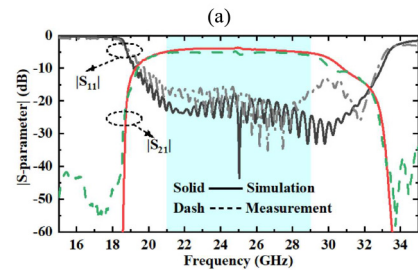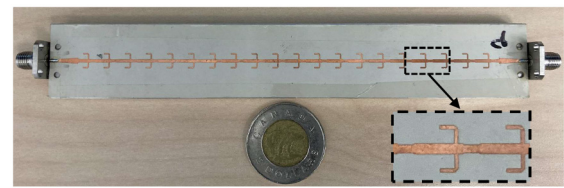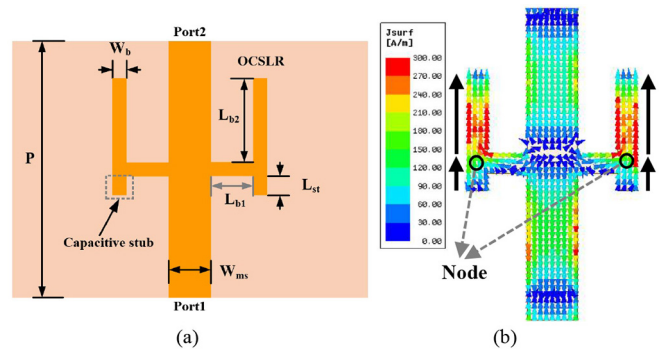
shifted toward a lower frequency by increasing the length of the loaded capacitive stub. The reason for this mode-shifting phenomenon can be simply explained by the fact that both the bend discontinuity and the loaded short stub behave like a shunt-capacitor [33]. They will increase the effective capacitance of the *RLC* series resonator circuit representing the 3rd mode (series-resonance), and thus lower the related resonance frequency. It is necessary to mention that the loaded capacitive stub will also introduce a radiating
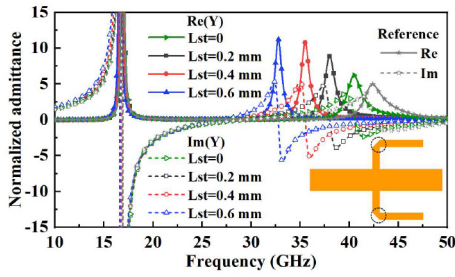
FIGURE 16. Dimensional effects of the short capacitive stub on the normalized admittance of the OCSLR. The curves marked as "Reference" represent the special case removing both the bend discontinuity and short capacitive stub, i.e., the one similar to the proposed OCUIR with a corner cut (as shown in the inset).
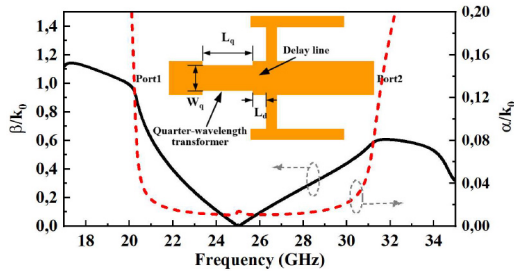

FIGURE 17. Normalized phase and attenuation constants of the proposed OCSLR-based microstrip combline LWA. Open-stopband issue is effectively suppressed by using a delay line and quarter-wavelength impedance transformer [10], as shown in the inset. Dimensions of them are L_d = 0.58 mm, L_q = 1.74 mm, and W_q = 0.65 mm.

edge involved into the total radiation mechanism; this is the second aspect that should be noticed for the proposed design. Thus, for the sake of radiation purity, this loaded short capacitive stub should be placed collinearly with the longer segment (i.e., the part that is parallel to the host line). In this case, the fringing fields of the loaded short stub's radiating edge will interestingly share the same direction with that of the folded OCUIR. This is because at the bend point (the "node"), the loaded short stub is capacitive while the longer segment of the folded OCUIR normally behaves inductively. At such "node" they will share the same electrical potential and hence their current directions will be totally reversed with respect to the "node". Namely one flows inward while the other flows outward of the "node", as displayed in Fig. 15(b) which illustrates the typical current distributions of the OCSLR. Consequently, it is concluded that the loaded short capacitive stub is able to play a significant role in the flexible mode-control of the proposed folded OCSLR yet without contaminating the overall radiation performances. In this context, the proposed OCSLR-based LWA is also capable of providing such good design freedoms and multifunctional electrical performances analogous to the above demonstrated ALSSP-based LWA. These would not be repeated here just for brevity. Fig. 17 depicts the normalized complex propagation constants of the proposed OCSLR-based LWA, where similar matching techniques as those in the OCUIR-based counterpart are also employed to suppress the open-stopband issue. The attenuation constant is not only kept relatively stable across the frequency band from

21 to 29 GHz, but also exhibits an obvious value improvement compared to the OCUIR counterpart shown in Fig. 13. For verification purposes, 20 OCSLR-related unit cells are cascaded to form a microstrip combline LWA, and the fabricated prototype is shown in Fig. 18(a). Fig. 18(b) shows its simulated and measured S-parameters, illustrating that a good impedance matching is achieved without presenting an open-stopband issue. We are more interested in the $|S_{21}|$ performance, which shows a stable curve pattern in the target frequency band from 21 to 29 GHz. Meanwhile, a larger insertion loss (i.e., improved radiation capability) can be found compared to Fig. 14(b), thanks to the flexible mode-control induced by the loaded capacitive stub and the shortened frequency-distance between the two series-resonances as indicated in Fig. 3. More importantly, an obvious filtering behavior with good out-of-band rejection is obtained. The radiation efficiency of the proposed OCSLR-based LWA is already depicted in Fig. 14(c). Not only is the stable efficiency realized (i.e., 74.3±7.2 %) that is consistent with such a $|S_{21}|$ curve pattern, but an apparent efficiency enhancement of about 15% than that of the OCUIR-based LWA is observed. The simulated and measured realized gain and beam-direction are displayed in Fig. 18(c). The simulated results suggest that an average gain of about 16.8 dBi with variation of ±1.8 dBi is realized in the frequency range from 21 to 29 GHz, where the beam-scanning span is from −40° (backward) to 20° (forward). The measured gain reasonably agrees with its simulated counterpart except for a little drop that may be due to an increased material losses and measurement tolerances, with a stable trend still remained (i.e., 16.5±1.5 dBi). Simulated and measured radiation patterns at several frequencies are shown in Fig. 19, indicating that a reasonable agreement is realized between the two cases with a slight difference that may be caused by fabrication errors or measurement issues. Notably, the simulated cross-polar components are too small to be visible.

V. DISCUSSION AND COMPARISON
So far, two types of 1-D periodic LWAs based on different transmission line technologies and RDs, i.e., ALSSP-based SIW LWA and SLR-based microstrip LWA have been elaborately studied. Thanks to the flexible mode-control capability owned by their RDs, good design freedoms and multifunctionalities in terms of circuit and radiation performances including controllable bandwidth/filtering characteristics, manageable beamwidth, and radiation stability have been achieved. However, there is a limitation behind this design concept when it comes to the achievable bandwidth and beamwidth of the related LWA: a larger beamwidth is always accompanied by a narrower bandwidth (or beam-scanning range), as revealed in Fig. 9. This is because increasing the attenuation constant and thus the beamwidth of the LWA simply relies on shorting the frequency distance between the two strong resonances of the relevant RD so as to enhance the absolute resistance/conductance value of the RD. Fortunately, the characteristic impedance/admittance

TABLE 1. A comparison between the proposed work and several references.

| Ref.	Operating Bandwidth	Beam-Scanning Range	Maximum Gain & Variation (dBi)	Radiating Discontinuity	Unit Cell Characteristic	Flexible Mode-Control Capability	Controllable Filtering Capability
[5]	16.2% (10.2-12 GHz)	15°–72°	14 (8)	Slot (SIW)	SMR-based unit cell	No	No
[7]	34.2% (8.5-12 GHz)	-70°–60°	13.5 (5)				
[11]	39.8% (13-19.5 GHz)	-48°–35°	14 (3)	Stub (Microstrip)	Composite unit cell		
[12]	52.9% (12.5-21.5 GHz)	-56°–75°	15 (3)				
[22]	16.9% (27-32 GHz)	4°–20°	16.6 (3)	ME dipole (SIW)	MMR-based unit cell		
[24]	28.6% (30-40 GHz)	-43°–28°	15.1 (2.6)				
[31]	24% (22-28 GHz)	-44°–40°	12.5 (2.8)	Patch (Microstrip)	SMR-based unit cell		Yes
[32]	4.5% (30.4-31.8 GHz)	18°–60°	12.1 (9)	Slot (SIW)			
OCSLR-based LWA	32% (21-29 GHz)	-40°–20°	18 (3)	Stub (Microstrip)	MMR-based unit cell	Yes	Yes
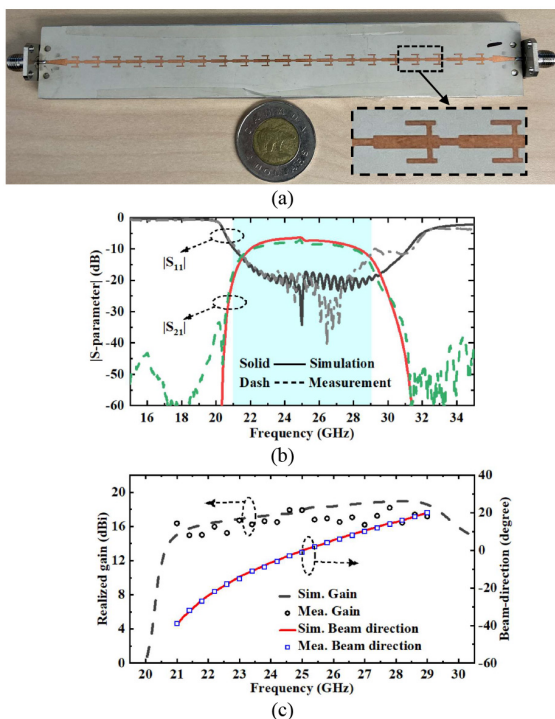
FIGURE 18. (a) Fabricated prototype of the proposed OCSLR-based microstrip combline LWA. (b) Simulated and measured S-parameters. (c) Simulated and measured realized gain and beam-direction.

FIGURE 19. Normalized radiation patterns of the proposed OCSLR-based microstrip combline LWA. (a) 22 GHz; (b) 25 GHz; (c) 28 GHz.

of the host TLs, according to equation (2), can also be exploited as an additional parameter to control the attenuation constant and thus beamwidth of the LWA. Besides, the width of the slot/stub in our proposed LWAs can be used as well to adjust the absolute resistance/conductance value of the RD without significantly influencing its resonance frequencies as mentioned before. In this sense, a fixed bandwidth can be realized by controlling the locations of the RD's tw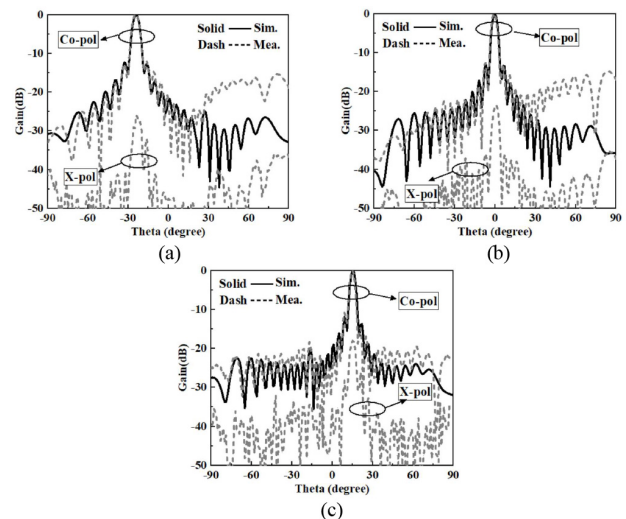o strong resonances, while the beamwidth can be conveniently tailored by suitably selecting the characteristic impedance/admittance of host TLs and/or the width of the slot/stub RD. Consequently, the proposed LWAs can be of more freedoms and versatilities when customizing their electrical performances in terms of beamwidth and bandwidth.

In order to highlight the benefits of our proposed LWAs using the flexible mode-control principle, a comparison has been conducted and tabulated as displayed in Table 1. Here, the proposed SLR-based microstrip LWA is selected as a representative of our works; then, it is used to compare with other references. It can be observed that compared to those SMR-related works [5], [7], the proposed SLR-based LWA is capable of simultaneously providing both the radiation stability and controllable filtering characteristics thanks to the MMR design rule together with the flexible

mode-control principle. The advantages of such two functionalities in the proposed SLR-based LWA are still sustained when compared with those works aimed for either radiation stability [11], [12], [22], [24] or controllable filtering capability [31], [32]. In addition to these, it also should be noted that a systematic or strategic approach to design an LWA with rich freedoms and versatilities in terms of circuit and radiation characteristics has been uniquely investigated in our work compared to others in the table. Thanks to these benefits, the proposed antennas, especially the OCSLR-based microstrip LWA, may potentially be a competent candidate or standard scheme to substitute those traditional counterparts as shown in Fig. 10(a) and (b) in practical system applications that, for example, need different bandwidths and beamwidths.

VI. CONCLUSION

In this paper, a class of single-layered multifunctional LWAs exhibiting flexibly engineered radiation and filtering characteristics, with the aid of mode-control principle, have been systematically explored and developed for microwave and millimeter-wave applications. It is demonstrated that by properly controlling the modal behaviors of the RD, the related LWAs can be freely tailored with respect to its attenuation constant while simultaneously maintaining radiation stability and possessing filtering behaviors. Aimed for different system-integration platforms, both microstrip and SIW transmission-line technologies are separately employed to implement LWAs whose RDs possess flexible mode-control capabilities. In addition to those desirable electrical performances as mentioned above, the proposed LWAs also have some merits from the perspective of industrial practicability, e.g., good design flexibilities and versatilities, single-layer, low-cost, easy fabrication/integration. Therefore, they may be a good candidate for practical system applications such as 5G communication and the IoV.

REFERENCES

[1] A. A. Oliner and D. R. Jackson, "Leaky-wave antenna" in *Antenna Engineering Handbook*, 4th ed., J. Volakis, Ed. New York, NY, USA: McGraw-Hill, 2007.

[2] C. Caloz, D. R. Jackson, and T. Itoh, "Leaky-wave antennas" in *Frontiers in Antennas—Next Generation Design & Engineering*, F. B. Gross, Ed. New York, NY, USA: McGraw-Hill, 2011.

[3] L. Wang, J. L. G.-Tornero, and O. Q.-Teruel, "Substrate integrated waveguide leaky-wave antenna with wide bandwidth via prism coupling," *IEEE Trans. Microw. Theory Techn.*, vol. 66, no. 6, pp. 3110–3118, Jun. 2018.

[4] A. Grbic and G. V. Eleftheriades, "Leaky CPW-based slot antenna arrays for millimeter-wave applications," *IEEE Trans. Antennas Propag.*, vol. 50, no. 11, pp. 1494–1504, Nov. 2002.

[5] J. Liu, D. R. Jackson, and Y. Long, "Substrate integrated waveguide (SIW) leaky-wave antenna with transverse slots," *IEEE Trans. Antennas Propag.*, vol. 60, no. 1, pp. 20–29, Jan. 2012.

[6] D. Zheng, Y.-L. Lyu, and K. Wu, "Transversely slotted SIW leaky-wave antenna featuring rapid beam-scanning for millimeter-wave applications," *IEEE Trans. Antennas Propag.*, vol. 68, no. 6, pp. 4172–4185, Jun. 2020.

[7] Y. Dong and T. Itoh, "Composite right/left-handed substrate integrated waveguide and half mode substrate integrated waveguide leaky-wave structures," *IEEE Trans. Antennas Propag.*, vol. 59, no. 3, pp. 767–775, Mar. 2011.

[8] Y. Geng, J. Wang, Y. Li, Z. Li, M. Chen, and Z. Zhang, "High-efficiency leaky-wave antenna array with sidelobe suppression and multibeam generation," *IEEE Antennas Wireless Propag. Lett.*, vol. 16, pp. 2787–2790, 2017.

[9] J. Liu, D. R. Jackson, Y. Li, C. Zhang, and Y. Long, "Investigation of SIW leaky-wave antenna for endfire-radiation with narrow beam and sidelobe suppression," *IEEE Trans. Antennas Propag.*, vol. 62, no. 9, pp. 4489–4497, Sep. 2014.

[10] J. T. Willianm, P. Baccarelli, S. Paulotto, and D. R. Jackson, "1-D combline leaky-wave antenna with the open stopband suppressed design considerations and comparisons with measurements," *IEEE Trans. Antennas Propag.*, vol. 61, no. 9, pp. 4184–4492, Sep. 2013.

[11] Y.-L. Lyu, F.-Y. Meng, G.-H. Yang, P.-Y. Wang, Q. Wu, and K. Wu "Periodic leaky-wave antenna based on complementary pair of radiation elements," *IEEE Trans. Antennas Propag.*, vol. 66, no. 9, pp. 4503–4515, Sep. 2018.

[12] Y.-L. Lyu, F.-Y. Meng, G.-H. Yang, Q. Wu, and K. Wu, "Leaky-wave antenna with alternately loaded complementary radiation elements," *IEEE Antennas Wireless Propag. Lett.*, vol. 17, no. 4, pp. 679–683, Apr. 2018.

[13] D. K. Karmokar, Y. J. Guo, P.-Y. Qin, S.-L. Chen, and T. S. Bird, "Substrate integrated waveguide-based periodic backward-to-forward scanning leaky-wave antenna with low cross-polarization," *IEEE Trans. Antennas Propag.*, vol. 66, no. 8, pp. 3846–3856, Aug. 2018.

[14] Z. Li, Y. J. Guo, S.-L. Chen, and J. Wang, "A period-reconfigurable leaky-wave antenna with fixed-frequency and wide-angle beam scanning," *IEEE Trans. Antennas Propag.*, vol. 67, no. 6, pp. 3720–3732, Jun. 2019.

[15] D.-F. Guan, Q. Zhang, P. You, Z.-B. Yang, Y. Zhou, and S.-W. Yong, "Scanning rate enhancement of leaky-wave antennas using slow-wave substrate integrated waveguide structure," *IEEE Trans. Antennas Propag.*, vol. 66, no. 7, pp. 3747–3757, Jul. 2018.

[16] Q. Zhang, Q. Zhang, and Y. Chen, "High-efficiency circularly polarized leaky-wave antenna fed by spoof surface plasmon polaritons," *IET Microw. Antennas Propag.*, vol. 11, no. 10, pp. 1639–1644, May 2018.

[17] N. Boskovic, B. Jokanovic, and M. Radovanovic, "Printed frequency scanning antenna arrays with enhanced frequency sensitivity and sidelobe suppression," *IEEE Trans. Antennas Propag.*, vol. 65, no. 4, pp. 1757–1764, Apr. 2017.

[18] D. S.-Escuderos, M. F.-Bataller, J. I. Herranz, and M. Cabedo-Fabrés, "Periodic leaky-wave antenna on planar goubau line at millimeter-wave frequencies," *IEEE Antennas Wireless Propag. Lett.*, vol. 12, pp. 1006–1009, 2013.

[19] J. R. James and A. Henderson, "A critical review of millimeter planar arrays for military applications," in *Proc. Military Microw. Conf.*, London, U.K., Oct. 1982, pp. 487–492.

[20] J. Y. Yin *et al.*, "Frequency-controlled broad-angle beam-scanning of patch array fed by spoof surface plasmon polaritons," *IEEE Trans. Antennas Propag.*, vol. 64, no. 12, pp. 5181–5189, Dec. 2016.

[21] L. Liu, M. Chen, J. Cai, X. Yin, and L. Zhu, "Single-beam leaky-wave antenna with lateral continuous scanning functionality based on spoof surface plasmon transmission line," *IEEE Access*, vol. 9, pp. 25225–25231, 2019.

[22] K.-M. Mak, K.-K. So, H.-W. Lai, and K.-M. Luk, "A magnetoelectric dipole leaky-wave antenna for millimeter-wave application," *IEEE Trans. Antennas Propag.*, vol. 65, no. 12, pp. 6395–6402, Dec. 2017.

[23] G. Zhang, Q. Zhang, S. Ge, Y. Chen, and R. D. Murch, "High scanning-rate leaky-wave antenna using complementary microstrip-slot stubs," *IEEE Trans. Antennas Propag.*, vol. 67, no. 5, pp. 2913–2922, May 2019.

[24] D. Zheng and K. Wu, "Leaky-wave antenna featuring stable radiation based on multimode resonator (MMR) concept," *IEEE Trans. Antennas Propag.*, vol. 68, no. 3, pp. 2016–2030, Mar. 2020.

[25] L. Chettri and R. Bera, "A comprehensive survey on Internet of Things (IoT) toward 5G wireless systems,' *IEEE Internet Things J.*, vol. 7, no. 1, pp. 16–32, Jan. 2020.

[26] R. Lu, L. Zhang, J. Ni, and Y. Fang, "5G vehicle-to-everything services: Gearing up for security and privacy," *Proc. IEEE*, vol. 108, no. 2, pp. 378–389, Feb. 2020.

[27] H. Zhou, W. Xu, J. Chen, and W. Wang, "Evolutionary V2X technologies toward the Internet of Vehicles: Challenges and opportunities," *Proc. IEEE*, vol. 108, no. 2, pp. 308–323, Feb. 2020.

[28] A. Hommes, A. Shoykhetbrod, and N. Pohl, "A fast tracking 60 GHz radar using a frequency scanning antenna," in *Proc. 39th Int. Conf. Infrared Millimeter Terahertz Waves (IRMMW-THz)*, 2014, pp. 1–2.

[29] A. Shoykhetbrod, T. Geibig, A. Hommes, R. Herschel, and N. Pohl, "Concept for a fast tracking 60 GHz 3D-radar using frequency scanning antennas," in *Proc. 41st Int. Conf. Infrared Millimeter Terahertz Waves (IRMMW-THz)*, 2016, pp. 1–3.

[30] F. Queudet, B. Froppier, Y. Mahe, and S. Toutain, "Study of a leaky waveguide for the design of a filtering antennas," in *Proc. IEEE Eur. Microw. Conf.*, Munich, Germany, Oct. 2003, pp. 943–946.

[31] M. H. Rahmani and D. Deslandes, "Circularly polarized periodic leaky-wave antenna with filtering capability," *IET Microw. Antennas Propag.*, vol. 12, no. 11, pp. 1811–1815, May 2018.

[32] D. Zheng and K. Wu, "Multifunctional filtering leaky-wave antenna exhibiting simultaneous rapid beam-scanning and frequency-selective characteristics based on radiative bandpass filter concept," *IEEE Trans. Antennas Propag.*, vol. 68, no. 8, pp. 5842–5854, Aug. 2020.

[33] R. E. Collin, *Foundations for Microwave Engineering*, 2nd ed. New York, NY, USA: McGraw-Hill, 1992.

[34] C. Balanis, *Antenna Theory: Analysis and Design*, 3rd ed. New York, NY, USA: Wiley, 2005.

[35] W. M. Abdel-Wahab and S. Safavi-Naeini, "Wide-bandwidth 60-GHz aperture-coupled microstrip patch antennas (MPAs) fed by substrate integrated waveguide (SIW)," *IEEE Antennas Wireless Propag. Lett.*, vol. 10, pp. 1003–1005, 2011.

[36] N. Marcuvitz, *Waveguide Handbook* (MIT Radiation Laboratory Series). New York, NY, USA: McGraw-Hill, 1951.

[37] S. X. Ta, H. Choo, I. Park, and R. W. Ziolkowski, "Multi-band, wide-beam, circularly polarized, crossed, asymmetric barbed dipole antennas for GPS applications," *IEEE Trans. Antennas Propag.*, vol. 61, no. 11, pp. 5771–5775, Nov. 2013.

[38] A. Karar, A. Ghosh, A. Chakraborty, S. R. Chowdhury, J. Chatterjee, and M. Chakrabarti, "Broadbanding of substrate integrated waveguide based slotted array antenna using dual slot configuration," in *Proc. 4th Int. Conf. Opto-Electr. Appl. Opt.*, 2017, pp. 1–5.

[39] R. Garg, P. Bhartia, I. Bahl, and A. Ittipiboon, *Microstrip Antenna Design Handbook*. Boston, MA, USA: Artech House, 2001.

[40] Q. Liao and L. Wang, "Switchable bidirectional/unidirectional LWA array based on half-mode substrate integrated waveguide," *IEEE Antennas Wireless Propag. Lett.*, vol. 19, no. 7, pp. 1261–1265, Jul. 2020.

[41] N.-W. Liu, L. Zhu, W.-W. Choi, and X. Zhang, "A low-profile aperture-coupled microstrip antenna with enhanced bandwidth under dual resonance," *IEEE Trans. Antennas Propag.*, vol. 65, no. 3, pp. 1055–1062, Mar. 2017.

[42] W.-J. Lu and L. Zhu, "Wideband stub-loaded slotline antennas under multi-mode resonance operation," *IEEE Trans. Antennas Propag.*, vol. 63, no. 2, pp. 818–828, Feb. 2015.

[43] X. Y. Zhang, J.-X. Chen, Q. Xue, and S.-M. Li, "Dual-band bandpass filters using stub-loaded resonators," *IEEE Microw. Wireless Compon. Lett.*, vol. 17, no. 8, pp. 583–585, Aug. 2007.

KE WU (Fellow, IEEE) received the B.Sc. degree (with Distinction) in radio engineering from the Nanjing Institute of Technology (currently Southeast University), China, in 1982, the D.E.A. degree from the Institut National Polytechnique de Grenoble in 1984, and Ph.D. degree (with Distinction) in optics, optoelectronics, and microwave engineering from the University of Grenoble, France, in 1987.

He is a Professor of Electrical Engineering and the NSERC-Huawei Industrial Research Chair of Future Wireless Technologies with the Polytechnique Montréal (University of Montreal), Montreal, QC, Canada. He has been the Director of the Poly-Grames Research Center. He was the Founding Director of the Center for Radiofrequency Electronics Research of Quebec (Regroupement stratégique of FRQNT) and the Tier-I Canada Research Chair of RF and Millimeter-Wave Engineering. He is currently with the School of Information Science and Engineering, Ningbo University, on leave from his home institution. He has held guest, visiting, and honorary professorships with many universities around the world. He has authored or coauthored over 1300 referred papers and a number of books/book chapters. He has filed more than 50 patents. His current research interests involve substrate integrated circuits and systems, antenna arrays, field theory and joint field/circuit modeling, ultra-fast interconnects, wireless power transmission and harvesting, and MHz-through-THz technologies and transceivers for wireless sensors and systems as well as biomedical applications. He is also interested in the modeling and design of microwave and terahertz photonic circuits and systems.

Dr. Wu was a recipient of many awards and prizes, including the first IEEE MTT-S Outstanding Young Engineer Award, the 2004 Fessenden Medal of the IEEE Canada, the 2009 Thomas W. Eadie Medal of the Royal Society of Canada, the Queen Elizabeth II Diamond Jubilee Medal in 2013, the 2013 FCCP Education Foundation Award of Merit, the 2014 IEEE MTT-S Microwave Application Award, the 2014 Marie-Victorin Prize (Prix du Quebec—the highest distinction of Québec in the natural sciences and engineering), the 2015 Prix d'Excellence en Recherche et Innovation of Polytechnique Montréal, the 2015 IEEE Montreal Section Gold Medal of Achievement, and the 2019 IEEE MTT-S Microwave Prize. He has held key positions in and has served on various panels and international committees, including the Chair of Technical Program Committees, International Steering Committees, and international conferences/symposia. In particular, he was the General Chair of the 2012 IEEE Microwave Theory and Techniques (IEEE MTT-S) International Microwave Symposium. He has served on the Editorial/Review Boards of many technical journals, transactions, proceedings and letters as well as scientific encyclopedia, including an editor and a guest editor. He was the Chair of the joint IEEE Montreal Chapters of MTT-S/AP-S/LEOS and then the restructured IEEE MTT-S Montreal Chapter, Canada. He has served IEEE MTT-S and Administrative Committee (AdCom) as the Chair of the IEEE MTT-S Transnational Committee, Member and Geographic Activities Committee, Technical Coordinating Committee, and 2016 IEEE MTT-S President among many other AdCom functions. He is currently the Chair of the IEEE MTT-S Inter-Society Committee. He is the inaugural representative of North America as a member of the European Microwave Association General Assembly. He was an IEEE MTT-S Distinguished Microwave Lecturer from 2009 to 2011. He is a Fellow of the Canadian Academy of Engineering and the Royal Society of Canada (The Canadian Academy of the Sciences and Humanities). He is a member of Electromagnetics Academy, Sigma Xi, URSI, and IEEE-Eta Kappa Nu (IEEE-HKN).

DONGZE ZHENG (Graduate Student Member, IEEE) was born in Bozhou, Anhui, China, in 1993. He received the B.S. degree from Anhui University, Hefei, Anhui, in 2014, and the M.E. degree from the South China University of Technology (SCUT), Guangzhou, China, in 2017. He is currently pursuing the Ph.D. degree with the Polytechnique Montréal (University of Montréal), Montreal, QC, Canada. He was the Outstanding Graduate in Anhui province. His master thesis was one of the excellent theses in the SCUT. He has authored/coauthored more than 20 academic journal and conference papers. His research interests include leaky-wave antennas, periodic structures, artificial transmission lines, wideband antennas, circularly polarized antennas, filters, and FMCW radars as well as radar signal processing. He currently serves as a Reviewer for several international journals, such as IEEE TRANSACTIONS ON ANTENNAS AND PROPAGATION, IEEE ANTENNAS AND WIRELESS PROPAGATION LETTERS, and IEEE ACCESS.